

# UC San Diego

## UC San Diego Previously Published Works

### Title

hESC Differentiation toward an Autonomic Neuronal Cell Fate Depends on Distinct Cues from the Co-Patterning Vasculature

### Permalink

<https://escholarship.org/uc/item/6978g6n7>

### Journal

Stem Cell Reports, 4(6)

### ISSN

2213-6711

### Authors

Acevedo, Lisette M  
Lindquist, Jeffrey N  
Walsh, Breda M  
et al.

### Publication Date

2015-06-01

### DOI

10.1016/j.stemcr.2015.04.013

Peer reviewed

# hESC Differentiation toward an Autonomic Neuronal Cell Fate Depends on Distinct Cues from the Co-Patterning Vasculature

Lisette M. Acevedo,<sup>1,2,4</sup> Jeffrey N. Lindquist,<sup>1,2</sup> Breda M. Walsh,<sup>1</sup> Peik Sia,<sup>1</sup> Flavio Cimadamore,<sup>2</sup> Connie Chen,<sup>2</sup> Martin Denzel,<sup>2</sup> Cameron D. Pernia,<sup>2,3</sup> Barbara Ranscht,<sup>2</sup> Alexey Terskikh,<sup>2</sup> Evan Y. Snyder,<sup>2,3,5,\*</sup> and David A. Cheresch<sup>1,3,4,\*</sup>

<sup>1</sup>Moore's Cancer Center, University of California, San Diego, La Jolla, CA, 92093, USA

<sup>2</sup>Sanford Burnham Medical Research Institute, La Jolla, CA 92037, USA

<sup>3</sup>Sanford Consortium for Regenerative Medicine, La Jolla, CA 92037, USA

<sup>4</sup>Department of Pathology, University of California, San Diego, La Jolla, CA 92093, USA

<sup>5</sup>Department of Pediatrics, University of California, San Diego, La Jolla, CA 92093, USA

\*Correspondence: [esnyder@sanfordburnham.org](mailto:esnyder@sanfordburnham.org) (E.Y.S.), [dcheresh@ucsd.edu](mailto:dcheresh@ucsd.edu) (D.A.C.)

<http://dx.doi.org/10.1016/j.stemcr.2015.04.013>

This is an open access article under the CC BY-NC-ND license (<http://creativecommons.org/licenses/by-nc-nd/4.0/>).

## SUMMARY

To gain insight into the cellular and molecular cues that promote neurovascular co-patterning at the earliest stages of human embryogenesis, we developed a human embryonic stem cell model to mimic the developing epiblast. Contact of ectoderm-derived neural cells with mesoderm-derived vasculature is initiated via the neural crest (NC), not the neural tube (NT). Neurovascular co-patterning then ensues with specification of NC toward an autonomic fate requiring vascular endothelial cell (EC)-secreted nitric oxide (NO) and direct contact with vascular smooth muscle cells (VSMCs) via T-cadherin-mediated homotypic interactions. Once a neurovascular template has been established, NT-derived central neurons then align themselves with the vasculature. Our findings reveal that, in early human development, the autonomic nervous system forms in response to distinct molecular cues from VSMCs and ECs, providing a model for how other developing lineages might coordinate their co-patterning.

## INTRODUCTION

For the human body to take shape and function properly, multiple cell types from different lineages and germ layers must interact with each other at the earliest stages of embryogenesis, coordinating their maturation, growth, and patterning. These processes persist throughout development and into adulthood. The obligate coordination of multiple cell and tissue types needed for the mature vertebrate body plan to emerge suggests a fundamental dynamic co-regulation. This process during human embryogenesis is not well understood (Robertson, 2004; Zacchigna et al., 2008). One prototypic example of a critical interaction between different lineages is the formation of the neurovascular unit in the nervous system. The widespread co-patterning of a mesoderm-derived vascular network with an ectoderm-derived neural network early in embryogenesis is central to the development of all organs that are not only appropriately innervated but also perfused via autonomously responsive vasculature (Glebova and Ginty, 2005).

The importance of neurovascular co-patterning is underscored by the number of phenotypes associated with malformation of these networks in knockout (KO) mice (Autiero et al., 2005) and humans (Rolle et al., 2003; Taguchi et al., 1994). In both the peripheral nervous system (PNS) and CNS, nerves and vasculature co-align to form intricate branching patterns (Quaegebeur et al., 2011).

However, little is known about the process by which this co-alignment is launched at the earliest stages of human embryogenesis. It is also unclear whether co-patterning mediates cell fate determination or vice versa and how the neural crest (NC, source of the PNS) and neural tube (NT, source of the CNS) contribute to co-patterning. Previous studies have concentrated on how CNS-derived signals such as semaphorins, ephrins, and netrins promote vascular development (Eichmann and Thomas, 2012; Tam and Watts, 2010) or how vascular-derived signals such as artemin and endothelin 3 promote axonal guidance (Glebova and Ginty, 2005; James and Mukoyama, 2011; Makita et al., 2008). These studies were typically performed in relatively late stages of development, not in the human epiblast, when the earliest critical fate and patterning determinations are made.

Human embryonic stem cells (hESCs), the *in vitro* representation of the human epiblast (Thomson et al., 1998), enable unique access to the spontaneous emergence of the three embryonic germ layers in culture (Itskovitz-Eldor et al., 2000), providing an opportunity to model and manipulate the earliest stages of human embryogenesis (Jakobsson et al., 2007; Wang et al., 1992). We developed a hESC differentiation model to examine the real-time emergence of the mesoderm-derived vascular and ectoderm-derived nervous systems. We observed that NC cells initiate neurovascular patterning based on cues from developing vascular endothelial cells (ECs) and smooth muscle

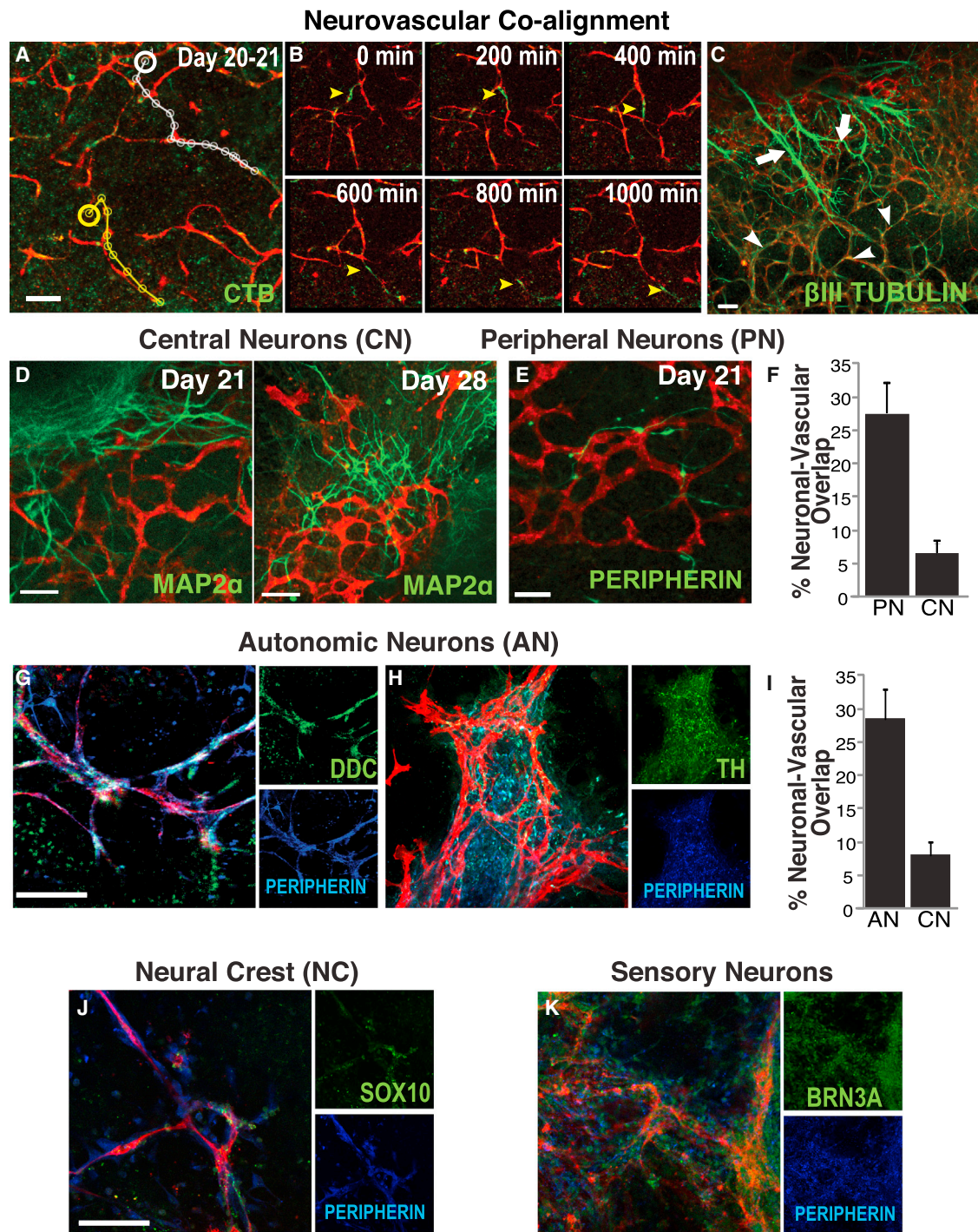


**Figure 1. Two Neuronal Populations Emerge from the Neuroectoderm, but Only Peripheral Neurons Initially Co-align with Developing BVs**

(A) ECs (*U.E.* lectin, red) and neuronal cells (cholera toxin [CTB], green) co-align. From [Movie S1](#), the tracks of two representative neuronal cells (yellow and white lines) are illustrated migrating along vascular networks from a set starting point (yellow and white circles).

(B) Shown are “snapshots” of association from days 20 to 21 at time points 0, 200, 400, 600, 800, and 1,000 min. Arrowheads denote neurons migrating along vessels.

(C–K) At day 21, there are two distinct populations of  $\beta$ III tubulin<sup>+</sup> neurons (green). One is associated with vascular networks (arrowheads); the other is independent of the vasculature (arrows). These are better distinguished in (D)–(K). CNs derived from the NT (MAP2 $\alpha$ , (legend continued on next page)



cells (VSMCs)—nitric oxide (NO) and T-cadherin, respectively. These events are required to drive co-patterned NC toward an autonomic fate. Once this neurovascular template is formed, then CNS neurites secondarily align with the existing vasculature.

## RESULTS

### Early Fate Determination and Co-Patterning of Blood Vessels and Autonomic Neurons Can Be Modeled Using hESCs

We hypothesized that neuronal and vascular structures may coordinate formation and patterning of their respective networks, accounting for their known juxtaposition and co-patterning in adult organisms (Suchting et al., 2006). To examine their emergence, we used what is regarded as a culture of the human epiblast, the pluripotent hESC, where all three germ layers emerge. To induce spontaneous heterogeneous differentiation, hESCs were grown in suspension as embryoid bodies (EBs) and plated on collagen type 1 in differentiation media to promote neovascularization (Kearney and Bautch, 2003; Lindquist et al., 2010). The EBs spread on the substrate to allow real-time microscopic visualization while maintaining critical 3D relationships. Over 28 days, we observed a gradient of iterative development with early blood vessel (BV) formation toward the periphery and maturation into lumen-containing VSMC-coated BVs toward the center (Figures S1A–S1G) (Lindquist et al., 2010). We also observed neuronal and vascular co-emergence, verified by kinetic analysis of gene expression. Early neuroectoderm markers (e.g., *PAX6*), late neural stem/progenitor cell markers (e.g., *nestin*), and more mature neuronal markers (e.g., *MAP2 $\alpha$* , *P75*, tyrosine hydroxylase [*TH*], and choline acetyltransferase [*CHAT*]) tracked with an upregulation of vascular endothelial (e.g., *CD31*) gene expression at days 14 and 21 (Figure S1H).

Live time-lapse confocal video microscopy imaging with *Ulex Europaeus* (*U.E.*) lectin and cholera toxin B (CTB) to label BVs and neurons, respectively, demonstrated that a

population of neurons migrated alongside vessels from days 7–14 (Figures 1A and 1B; Movie S1). CTB and the pan-early neuronal marker  $\beta$ III tubulin (Tuj1) showed  $73.5\% \pm 3.5\%$  overlap, confirming the specificity of CTB labeling (data not shown). At day 21, staining for *U.E.* lectin and  $\beta$ III tubulin revealed two distinct populations of primitive neurons emerging from the neuroectoderm contemporaneously with the developing vasculature (Figure 1C). One neuronal population co-migrated with the immature vessels (Figure 1C, arrowheads). The other population originated from the center where primitive NT-like structures are located and sent processes outward toward the vascular bed, but remained independent of the vascular pattern (Figure 1C, arrows). Similar results were observed with the pan-neuronal marker Neurofilament H (Figure S1I).

To determine which neurons were associated with newly formed BVs at this stage of development, we examined markers for CNS versus PNS neuronal populations. In day 21 hESC cultures, CNS neuron patterning defined by *MAP2 $\alpha$*  staining was independent of vascular patterning (Figure 1D). Instead, co-aligning neurons were positive for the NC-derived PNS neuronal marker peripherin (Figure 1E) and showed a 4-fold increase in overlap as compared with central neurons (CNs) (Figure 1F). By day 28, CNs had become associated with the vasculature (Figure 1D), suggesting that the well-established interactions between CNs and BVs may occur only after vessels have engaged with NC-derived peripherin<sup>+</sup> neurons. These peripherin<sup>+</sup> neurons also expressed the autonomic neuronal marker dopa decarboxylase (DDC) (Figure 1G) as well as other markers consistent with the catecholaminergic sympathetic (e.g., *TH*) (Figure 1H) or cholinergic parasympathetic (e.g., *CHAT*) (Figure S1K) function of the autonomic nervous system. DDC<sup>+</sup> neurons co-aligning with the vasculature were also positive for the neuronal marker HuC (Figure S1J). Based on this labeling pattern, we termed these cells autonomic neurons (ANs). Nuclear staining for MASH1 further identified these cells as early NC-derived ANs and confirmed that these nuclei were associated with migrating cell bodies rather than neurites

green) do not co-align with the vasculature (*U.E.* lectin, red) at day 21 (D, left); neurites from those neurons pursue a course largely independent of the vessels. The neurons that do co-align with vessels (*U.E.* lectin, red) at day 21 express the peripheral neuron (PN) marker peripherin (green) (E). Only after PNs begin to form a neurovascular pattern do central neurites begin to comport to that pattern (day 28) (D, right). (F) Co-localization of vasculature (*U.E.* lectin) with PNs (peripherin<sup>+</sup>) is 3.9-fold greater than with CNs (*MAP2 $\alpha$* ) (n = 9 images per group from three independent experiments). (G and H) These peripherin<sup>+</sup> (blue) neurons come to express the autonomic marker DDC (G, green) and TH (H, green). (Nuclei expressing the early autonomic transcription factor MASH1 in proximity with the vessels [Figure S1K] confirm that the cells themselves, and not just the processes of these incipient ANs, juxtapose with vessels). (I) Co-localization of vasculature (*U.E.* lectin) with NC-derived ANs (DDC<sup>+</sup>) is 4-fold greater than with NT-derived CNs (*MAP2 $\alpha$* ) (n = 10 images per group from three independent experiments). (J) Co-aligning neurons express SOX10 (green), confirming that they are NC derived. (K) Some express the sensory marker BRN3A (green), an alternative NC-derived PN phenotype (see text for caveats on emergence of this cell type). Scale bar represents 100  $\mu$ m for all images.

See Figure S1 for a description of the hESC differentiation model.



extending from CN somata (e.g., in the NT) (Figure S1K). Quantitative analysis of central (MAP2 $\alpha^+$ ) and autonomic (DDC $^+$ ) neurons in areas of hESC cultures where BVs were present indicated that ANs exhibited a 4-fold increase in overlap with the vasculature as compared with CNs (Figure 1I). Peripherin $^+$  neurons also stained positively for the NC markers SOX10 and P75 (Figures 1J and S1K), confirming that they were NC derived. Some of the peripherin $^+$  neurons co-expressed BRN3A (Figure 1K) and substance P (SubP) (Figure S1K), markers of sensory neurons, which were previously observed to associate with arteries (Mukouyama et al., 2002). The putative ANs did not express MPZ (myelin protein p0), ruling out the possibility that they may actually be migrant glia (Figure S1L).

### BVs Are Required for Peripheral Autonomic Neuronal Differentiation

We next considered whether AN cell fate commitment depended on the prior formation of BVs or vice versa. Neovascularization was significantly diminished by blocking the function of integrin  $\alpha v \beta 3$  (Cheresh, 1987) expressed on newly forming BVs (Figure S1D). This, in turn, reduced the AN (P75 $^+$  or DDC $^+$ ) population (Figures 2A and 2B). Importantly, MAP2 $\alpha^+$  CNs formed and persisted independently of the compromised vasculature (Figures 2A and 2B). In contrast, ablation of developing peripheral neurons with p75-saporin did not impact the emergence of ECs (Figure S2A); however, it did appear to inhibit further development, arresting them in a more immature less organized pattern and preserving a larger vessel diameter as seen in more primordial “mother vessels” (Figure S2B). These findings suggest that AN development and differentiation depend on the presence of a developing vasculature and that vascular maturation may also require association with NC-derived neurons.

To determine whether newly forming BVs are sufficient to promote the peripheral neuronal differentiation of NCs, we added exogenous hESC-derived NCs expressing GFP under a histone 2B promoter (Curchoe et al., 2010) to the maturing vascular structures in our hESC differentiation model at day 21. After 7 days, we detected a significant number of GFP $^+$  NCs that had attached and migrated along vascular networks (Figure 2D). Only those GFP $^+$  NCs in direct contact with BVs were peripherin $^+$  (Figure 2E), while NCs *not* in direct contact with vasculature remained undifferentiated (Figure S2C), suggesting that vascular association may be both necessary and sufficient to direct NCs toward ANs.

### hESC-Derived NC Differentiation toward an Autonomic Fate Depends on Association with ECs and VSMCs

BVs develop as endothelial tubes and then mature through recruitment of perivascular cells that include VSMCs.

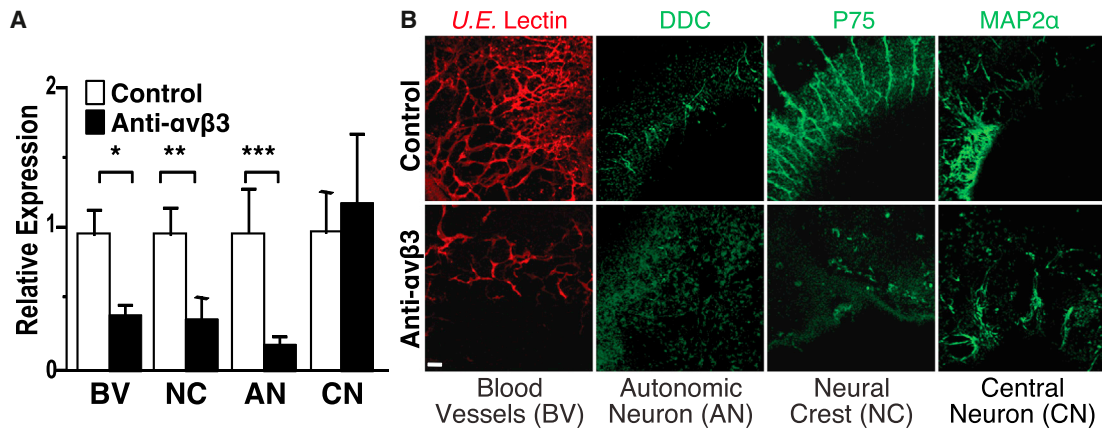
Although we observed that NCs associate with both VSMC-coated and -uncoated vessels, ANs innervate VSMCs to regulate vascular tone in the neurovascular unit in vivo. Therefore, we examined whether vascular maturation and/or the presence of VSMCs can impact autonomic neuronal differentiation. We embedded NCs in a 3D gel containing human primary ECs and VSMCs grown under conditions to promote the formation of VSMC-coated vascular tubes (Nakatsu et al., 2007; Scheppke et al., 2012). As in the hESC differentiation model (Figure 2D), NCs associated with vascular structures consisting of either ECs alone or those coated with VSMCs (Figure 3A). However, only NCs in contact with VSMC-coated vessels showed intense staining for  $\beta$ III tubulin and peripherin (Figures 3B and 3C, bottom). However, NCs in contact with vascular structures containing ECs alone displayed low levels of  $\beta$ III tubulin staining and lacked peripherin staining (Figures 3B and 3C, top), suggesting that commitment toward a PN fate occurs only when both ECs and VSMCs are present. Furthermore, NCs expressed significant levels of the autonomic marker DDC only when in contact with VSMC-coated vessels. In contrast, NCs contacting EC tubes lacking VSMCs expressed minimal levels of DDC (Figures 3D and 3F). *TH* and *MASH1* gene expression also increased when ECs and VSMCs were both present (data not shown). These results indicate that NC contact with VSMC-coated endothelial vascular structures drives them toward an autonomic fate and that *both* ECs and VSMCs are likely required for autonomic differentiation.

Sensory neurons, another NC-derivative, also interact with BVs in the mature human body plan and in our hESC differentiation model (Figure 1K). Interestingly, in the 3D reconstitution model, we observed BRN3A staining in NCs that were cultured with ECs *alone* but *not* in NCs co-cultured with both ECs and VSMCs, the condition apparently necessary for maximal AN marker expression (Figures S3A and S3B). Although NCs cultured with ECs alone were BRN3A $^+$ , the absence of peripherin staining and weak  $\beta$ III tubulin staining in these NCs (Figure S3A) suggests that these are not fully developed sensory neurons. Instead, additional differentiation cues may be required for commitment of these cells toward a sensory fate.

We next examined whether a 3D vascular structure was required for NC differentiation or whether the mere presence of ECs and VSMC in culture was sufficient to drive this process. As seen in the 3D model, NCs plated onto 2D monolayers containing ECs and VSMCs acquired AN marker expression (peripherin $^+$  and DDC $^+$ ) after 4–7 days in co-culture (Figure 3E). At day 7, 94.9%  $\pm$  6.0% of DDC $^+$  NC-derivatives were peripherin $^+$  (Figure S3C) and expressed TH, MASH1, and HuC, further supporting their differentiation toward ANs (Figures S3D and S3E). Therefore, a 3D vascular structure and/or lumenization appeared *not* to be required to



## Vascular Disruption



## Exogenous hES-derived NCs

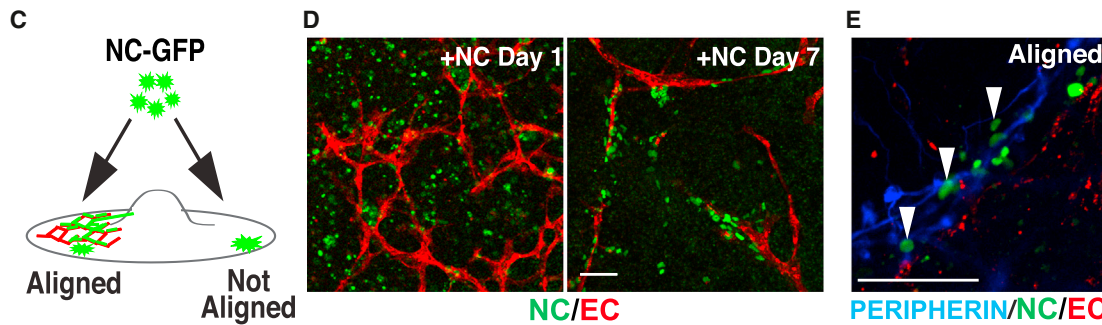


**Figure 2. Newly Forming BVs Are Necessary for Promoting NC Differentiation toward an AN Fate, but Not for the Emergence of CNs** (A and B) For “loss-of-function” studies, hESC cultures were treated with an integrin  $\alpha v \beta 3$  function-blocking antibody LM609 (which disrupts vascular development) or with a control IgG antibody and then stained for the presence of BVs (*U.E.* lectin, red), NC (p75, green), ANs (DDC, green), and CNs (MAP2 $\alpha$ , green). Disruption of vascular development compromises NC-derived AN differentiation or survival but has no impact on NT-derived CNS neurons. (A) The staining pixel area of hESC cultures was quantitated using Image J (left) ( $n = 6$  images per group from three independent experiments,  $*p = 0.005$ ,  $**p = 0.023$ ,  $***p = 0.034$ , error bars are  $\pm$  SEM). (B) Representative images of hESC cultures treated with control (top, right) or with the integrin  $\alpha v \beta 3$  function blocking antibody LM609 (bottom, right). (C) Schematic for one of the “gain-of-function” studies, illustrating the addition of H2B-GFP-labeled hESC-derived NC (NC-GFP) to the hESC-derived vascular culture system at day 21. After 7 days, NCs that came in contact with BVs co-aligned and differentiated, whereas NCs that came into contact with non-vascularized areas failed to align and differentiate. (D) Representative images of exogenously added NC-GFP cells (green) to the hESC differentiation model and their relation to vascular structures (*U.E.* lectin, red)—immediately after plating on day 1 (left) and after 7 days (right), during which interval the NCs-GFPs have aligned with the vasculature. (E) NCs (green), aligned with BVs (*U.E.* lectin, red), differentiated along a PN lineage (peripherin, blue) (arrowheads), while NCs that attached in avascular areas did not. See Figure S2 for the converse experiment, the adverse effect of NC disruption on vascular development, and maturation. Scale bar represents 100  $\mu$ m for all images.

drive NC commitment to an autonomic fate. Rather, the presence or absence of VSMCs in combination with ECs seemed to be critical for differential fate commitment.

### Direct Contact between NCs and VSMCs Is Required for Differentiation toward an Autonomic Fate

Because AN differentiation was only observed in areas of contact with both ECs and VSMCs, we examined the

requirement for direct cell-cell contact between the pertinent cell types by placing NCs, ECs, and VSMCs in the same or separate transwell chambers (Figures 4A and 4B). NCs were always plated in the top chamber (T). Culturing NCs in direct contact with VSMCs in the top chamber (T) and indirect contact with ECs in the bottom chamber (B) promoted autonomic differentiation (DDC<sup>+</sup>) in a manner similar to when all three were co-cultured in the same

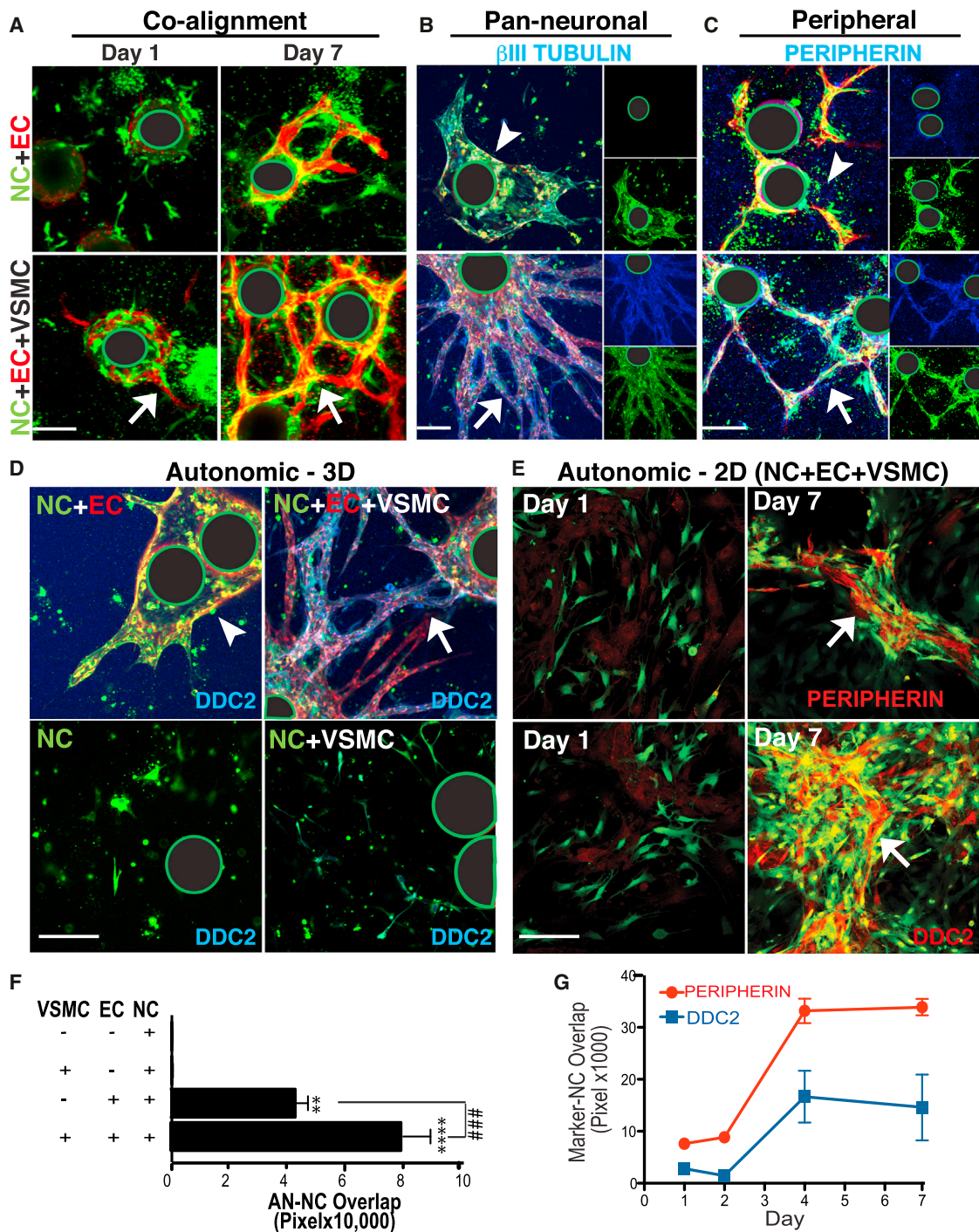


**Figure 3. Exogenously Added NCs Align with Vasculature to Assume an AN Fate if a VSMC Coating Is Present**

(A) hESC-derived NCs (DiI, green) embedded into 3D fibrin gels with EC (*U.E. lectin*, red)-coated beads co-align starting at day 1 (left, white arrow) becoming quite robust at day 7 (right, white arrow). (Note the green-encircled black regions in images represent the location of the Cytodex beads upon which ECs were coated [see [Experimental Procedures](#)].) Co-alignment of NCs with newly forming vessels occurs independently of the addition of VSMCs (top left), although the latter are required for robust vascular tube formation (bottom left, red). (B and C) Cells, under the various experimental conditions shown in (A), were stained for the co-expression of neuronal markers. Each large panel shows a merged image; the insets show the markers in separate channels. NCs (green) on VSMC-coated vessels (bottom panels) expressed (B) the pan-early neuronal marker βIII tubulin (blue) and (C) the PN marker peripherin (blue), much more strongly

(legend continued on next page)



chamber (Figures 4A and 4B). These NCs also expressed TH and peripherin. (Figure S4A). However, culturing NCs in direct contact with ECs (T) and indirect contact with VSMCs (B) failed to induce NC differentiation toward an autonomic fate (Figures 4A and 4B). These studies suggest a distinct mechanism for autonomic fate determination requiring NC cells in direct contact with VSMCs and indirect contact with ECs.

#### EC-Derived NO Is Required for AN Fate Determination

Although our findings suggest that direct contact between NCs and ECs is *not* required for autonomic differentiation, ECs are necessary. Pre-conditioning VSMCs by co-culturing them with ECs for 24 hr in a transwell system in which VSMCs were plated in the top chamber and ECs were plated in the bottom chamber and then removing the ECs prior to the addition of NCs did *not* lead to autonomic differentiation (Figure S4B). These observations suggest that sustained exposure to a factor (or factors) secreted by ECs may be required for NC differentiation toward an AN fate and that NCs, not VSMCs, are likely the primary target of that factor. One candidate that we examined was NO because it is a key regulator of the neurovascular unit. Furthermore, NO can promote neurogenesis (Chen et al., 2005; Reif et al., 2004; Carreira et al., 2012; Luo et al., 2010) and neuronal differentiation (Cheng et al., 2003; Oh et al., 2010). In our transwell model, ECs, which express endothelial NO synthase (eNOS), were treated with the NOS inhibitor L-NMMA, while VSMCs and NCs were plated together in the top chamber. We found that L-NMMA dose-dependently inhibited AN differentiation (Figure 4C). Similarly, knockdown of eNOS in ECs using transient siRNA transfection led to sharp reduction in DDC<sup>+</sup> cells (Figure 4D). To further explore the sufficiency of NO in AN differentiation, we cultured NCs in the presence of VSMCs and the NO

donor NOC-18 without ECs. Under these conditions, NO promoted AN differentiation (Figure 4E). Together these findings indicate that NO secreted by ECs is likely necessary and sufficient for promoting NC autonomic differentiation in the presence of VSMCs.

To determine whether NO secreted by ECs selectively promoted *autonomic* differentiation, we examined whether NO played a role in upregulating BRN3A expression when NCs are co-cultured with ECs alone (a condition previously noted to be sufficient to enable BRN3A expression, albeit without peripherin expression) (Figures S3F and S3G). In the transwell model, ECs drove BRN3A expression in NC regardless of whether the contact was direct or indirect (Figure S4C), and indeed, pharmacological and genetic inhibition of eNOS in ECs also decreased BRN3A<sup>+</sup> NCs (Figures S4D and S4E), suggesting that NO is required for general neuronal differentiation and is not a specific mediator of AN differentiation. These studies emphasize the unique role that direct contact between VSMCs and NCs plays in further refining the peripheral neuronal differentiation of NCs toward an AN fate.

#### T-Cadherin-Mediated Cell-Cell Contact between VSMC and NC Drive AN Differentiation

Our data reveal that direct contact between VSMCs and NCs is required for AN differentiation (Figure 4A). Therefore, to identify a direct contact mechanism that might mediate AN differentiation, we considered the cadherin family of membrane receptors because it acts as important regulators of cell-cell interactions between a wide array of cell types (Halbleib and Nelson, 2006). We examined the kinetic expression of E-, N-, R-, T-, and VE-cadherin in these cultures to determine whether expression of one or more of these molecules might be associated with emergence of the neurovascular unit. Only expression of T-cadherin (T-cad)

(white arrows) compared, respectively, to that seen in NCs cultured with ECs alone [top, B and C, white arrowheads], demonstrating a greater degree of neuronal marker upregulation when NCs were in the presence of both ECs and VSMCs (white arrows).

(D) The AN marker DDC (blue) is strongly upregulated in NCs (DiI, green) aligning with VSMC-coated vessels (*U.E.* lectin, red) (top right, white arrow), as compared to non-VSMC coated vessels (top left panel, white arrowhead), to NCs alone (bottom left), and to NCs co-cultured with only VSMCs (No ECs) (bottom right).

(E) NCs (green) plated in 2D on ECs and VSMCs (Day 1, left panels) strongly expressed peripherin (red) (top right, white arrow) as well as DDC (red) (bottom right panel, white arrow) by Day 7. Scale bar represents 100  $\mu$ m.

(F) Quantitation of co-localization (pixel overlap) of labeled NCs (green) and DDC expression (red), demonstrating that NCs expressed DDC (presumably differentiated into ANs) most robustly when in the presence of both VSMCs and ECs.  $94.9\% \pm 6.0\%$  of DDC<sup>+</sup> NC-derivatives were peripherin<sup>+</sup> (data not shown). Data presented as mean  $\pm$  SEM. A one-way ANOVA with Tukey's post-test was used to determine the difference in DDC staining among the following conditions: "NC only" (control) (n = 5 wells, 2 independent experiments), "EC+NC" (n = 8 wells, 4 independent experiments), "VSMC+NC" (n = 4 wells, 2 independent experiments), and "EC+VSMC+NC" (n = 9 wells, 4 independent experiments). ### indicates p = 0.0024 for EC+NC versus EC+VSMC+NC.

(G) Time course of AN differentiation, as determined by the co-expression (pixel overlap) of peripherin (red) or DDC (blue) and NCs (green) on days 1–7 (n = 10 images, 6 wells per group, 2 independent experiments). Expression of both peripherin and DDC peaks at day 4 and persists through day 7. Data presented as mean  $\pm$  SEM. A one-way ANOVA with Tukey's post-test was used to determine statistical significance. See Figure S3 for further data showing that exogenously added NCs align with vasculature to assume an AN fate only if VSMCs and ECs are present.





## NC Differentiation in Transwell Co-cultures

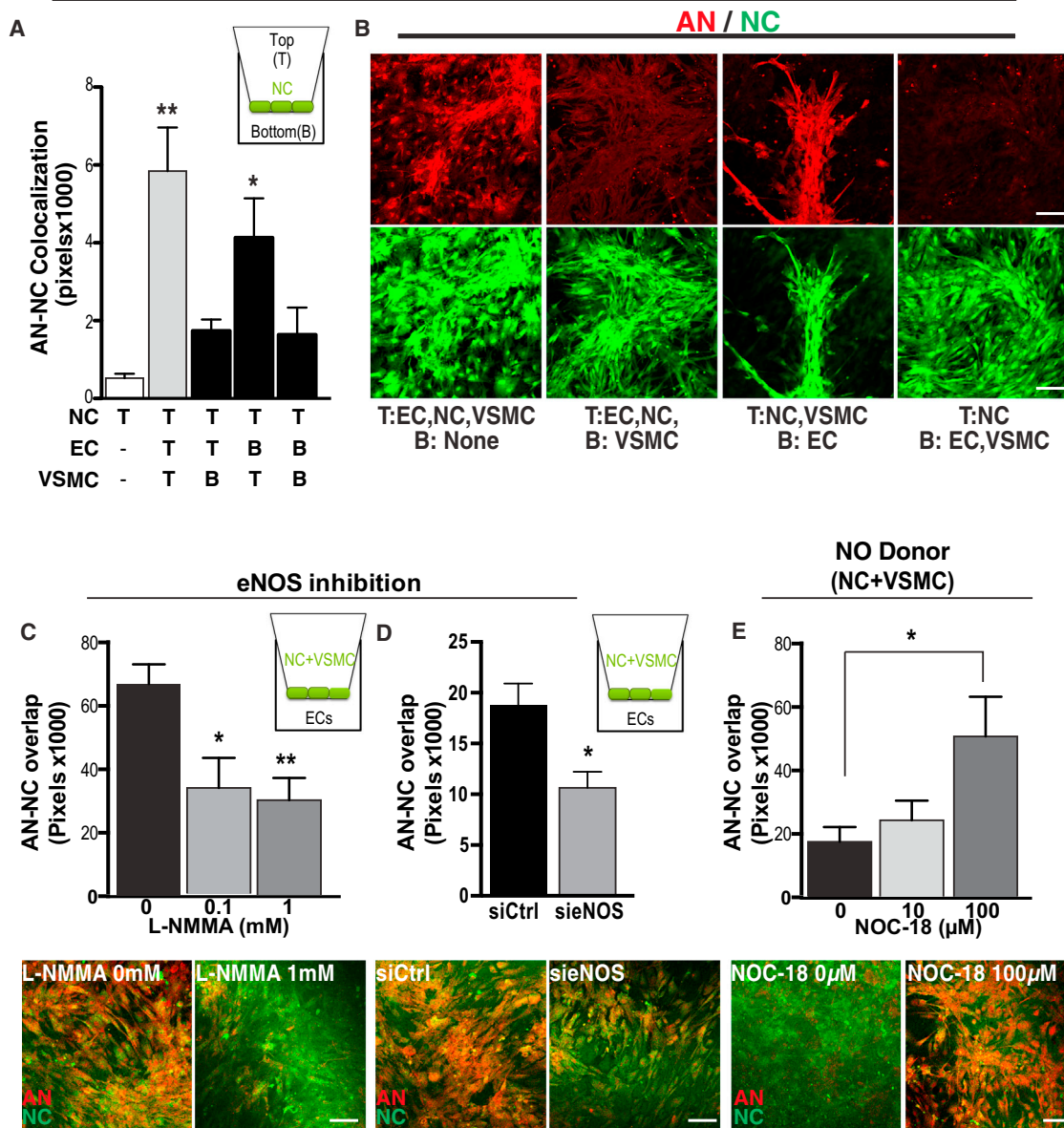


**Figure 4. NC Differentiation toward an AN Lineage Requires Both EC-Produced NO and Direct Contact with VSMCs**

(A and B) Direct contact between NC (DiI, green) and VSMCs is required for differentiation toward an AN lineage (DDC, red). (A) Quantitation of NC differentiation toward DDC<sup>+</sup> neurons (AN), as measured by co-localization (pixel overlap) of NC and DDC staining, when NCs are cultured in the top (T) chamber and ECs and/or VSMCs are cultured in either the top chamber (allowing cell-cell contact with the NCs) or bottom (B) chamber, allowing exposure of the NCs to only diffusible factors (diagramed in inset). Data presented as mean ± SEM. A one-way ANOVA with Dunnett's post-test was used to determine statistical significance from the NC only group (n = 6 wells, three independent experiments). \*\*p < 0.01, \*p < 0.05.

(B) Representative images of NCs co-cultured as described. The top are images of cells stained for the AN marker DDC. The bottom are images of NCs expressing DiI (green).

(C–E) EC-derived NO promotes AN differentiation, defined by an upregulation of DDC, as determined by loss-of-function (C and D) and gain-of-function (E) experiments. (C) DDC expression (red) decreased when NO production is inhibited. (Top) Quantitation of NC differentiation toward DDC<sup>+</sup> neurons after 5 days in co-culture (measured as above) when NCs and VSMCs are co-cultured in the top (T) chamber and ECs treated with L-NMMA (an inhibitor of NO production added to only the bottom chamber 1 hr prior to the addition of NCs and VSMCs) are cultured in the bottom (B) chamber (schematized in inset). Data presented as mean ± SEM. A one-way ANOVA with Dunnett's post-test was

(legend continued on next page)



and the endothelial marker VE-cadherin increased more than 2-fold between days 7 and 21, the period during which both neurons and BVs co-emerged in the hESC model. Expression of the epithelial marker E-cadherin decreased over time (Figure 5A), as expected (D'Amour et al., 2005). T-CAD was primarily expressed in areas where BVs and neurons were co-patterning (Figure 5B, arrowheads). We also observed its expression in ECs, VSMCs, and NCs in the 3D and 2D co-culture models (Figures 5C and 5D). T-cad expression was upregulated on NCs after 7 days in co-culture with ECs and VSMCs, when differentiation peaked (Figure 5D). These results point to T-cad as a potential regulator of AN differentiation and possibly one of the key adhesion molecules potentiating cell-cell contact between NC and VSMCs.

Physiologically, NC-derived ANs are known to align closely with BVs within the enteric nervous system of the gastrointestinal tract. Accordingly, we observed in both mouse and human intestinal tissue specimens that T-cad was coordinately expressed on BVs and NC-derived neurons (Figures 5E and 5F). In T-cad KO mice (Hebbard et al., 2008), there was a marked reduction in neuronal and vascular association relative to WT mice (Figures S5A and S5B). We observed a significant reduction of NC-derived neurons in the guts of T-cad KO mice compared with their littermate WT controls—a condition known clinically as a Hirschsprung's phenotype (or partial aganglionosis) (Figures S5B and S5C). Together, these findings support a role for T-cad in proper neurovascular co-alignment and consequent NC-derived neuronal prevalence.

To refine our investigation of how T-cad regulates vascular-mediated AN differentiation, we transiently knocked down T-cad in ECs, VSMCs, or NCs prior to embedding them in our 3D vascular tube model. Only loss of T-cad in NC or VSMCs led to a significant decrease in AN differentiation as measured by staining first with the pan-neuronal marker CTB (Figure 6A) and the AN marker DDC (Figure 6B). T-cad knockdown in ECs did not inhibit AN differentiation (Figures 6A and 6B). These find-

ings are consistent with a role for T-cad in direct cell-cell interactions between the VSMC and NC. Similarly, T-cad knockdown in VSMCs or NCs inhibited differentiation of NCs in the transwell model, whereas knockdown in ECs had no such effect (Figure S6B). To further investigate the role of T-cad in AN determination, we utilized a soluble form of recombinant T-cad (rT-cad) known to selectively disrupt T-cad-mediated cell-cell adhesion (Fredette et al., 1996). Because direct cell-cell contact between NCs and VSMCs is critical for AN differentiation (Figure 4A), we examined the interaction between these cells in the transwell model. Soluble rT-cad as a receptor antagonist was added to the top chamber at the time of NC and VSMC cell addition, and ECs were plated in the bottom chamber. After 4 days in co-culture, soluble rT-cad treatment significantly decreased the number of DDC<sup>+</sup> and peripherin<sup>+</sup> neurons, suggesting that NC differentiation toward an AN fate had been restricted (Figure 6C).

We next examined whether soluble rT-cad could negatively regulate the emergence of ANs in our hESC differentiation model where NCs spontaneously co-align with newly forming BVs. rT-cad added to hESC cultures during vascular and neuronal co-patterning (days 14–21) resulted in significantly fewer ANs associating with BVs (Figure 6D). These observations suggest that the initial T-cad-mediated interaction established at the time of NC-vasculature co-association is critical for driving NCs toward an AN lineage.

Taken together, our findings suggest that a homotypic direct interaction between T-cad on the surface of VSMCs and NCs in the presence of EC-derived secreted NO drives NC toward an AN fate thereby facilitating the earliest stages of functional neurovascular co-patterning in the human epiblast. From the perspective of the neuroectoderm, it is the NCs rather than the NT derivatives that drive this pivotal association with emerging vasculature. Once such a neurovascular pattern has been established, *then* neurites from CNs (derived from the NT) come to comport to that pre-established template.

---

used to determine statistical significance from control group (n = 9 wells, three independent experiments). \*p = 0.0494 \*\*p = 0.016. (Bottom) Representative images of co-cultures treated with either vehicle or L-NMMA (1 mM).

(D) DDC expression (red) decreased when eNOS was knocked down. (Top) Quantitation of NC differentiation toward DDC<sup>+</sup> neurons after 5 days in transwell co-cultures as described above (and schematized in inset). ECs were treated with 5 nM si-eNOS or control siRNA 12 hr prior to co-culture. Data are presented as mean ± SEM. A two-tailed Student's t test was used to determine statistical significance from si-Ctrl group (n = 5 wells, three independent experiments). \*p = 0.0016. (Bottom) Representative images of co-cultures treated with either siRNA control or si-eNOS (5 nM).

(E) The NO donor NOC-18 increases AN differentiation (DDC<sup>+</sup>) of NCs when cultured with VSMCs but without ECs. (Top) Quantitation of NC differentiation toward DDC<sup>+</sup> neurons (as described above). Data are presented as mean ± SEM. A one-way ANOVA with Dunnett's post-test was used to determine statistical significance from control group (n = 9 wells, three independent experiments). \*p = 0.0158. (Bottom panel) Representative images of co-cultures treated with either control (0 μM) or NOC-18 (100 μM). Scale bar represents 100 μm for all images.

See also Figure S4.

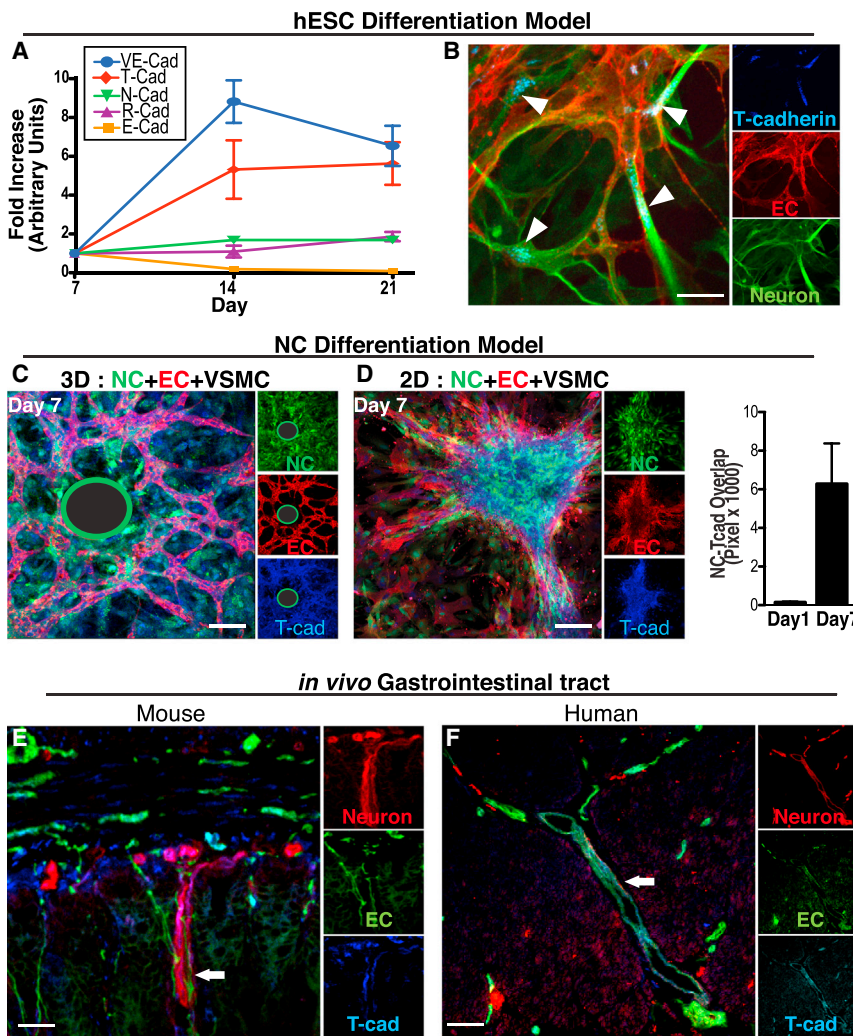


**Figure 5. T-CAD Is Expressed by Both Neurons and BVs at Peak Differentiation and Co-alignment**

(A) Q-PCR analysis of cadherin gene expression in the hESC differentiation model. *T-CAD* (red diamonds) expression is upregulated by day 14, when co-patterning is observed and when VE-cadherin (an EC marker) expression is highest (n = 2 replicates, two independent experiments).

(B) T-cad (blue) staining in the hESC differentiation model. T-cad is expressed on both ECs (*U.E.* lectin, red) and neurons ( $\beta$ III-tubulin, green) at day 21. Arrowheads denote T-cad localized to EC/neuronal junctions. Scale bars represent 25  $\mu$ m.

(C and D) T-cad (blue) is expressed in NCs (green) only when cultured with both ECs (*U.E.* lectin, red) and VSMCs in our NC differentiation model. This was observed in 3D (C) and 2D (D). (The green-encircled black regions represent the location of the Cytodex beads upon which ECs were coated in the 3D fibrin gel system; see [Supplemental Experimental Procedures](#)).

(D, right) Quantitation of NC (green) co-localization with T-CAD staining (blue) (based on overlap of pixels) increasing over time (n = 5 images, two independent experiments). Data are presented as mean  $\pm$  SEM. Scale bar represents 100  $\mu$ m.

(E) Immunostaining of mouse GI tract for T-cad (blue) on ECs (CD31, red) and neurons (L1, green).

(F) Immunostaining of human GI tract for T-cad (blue) on ECs (*U.E.* lectin, red) and neurons ( $\beta$ III tubulin, green). White arrow

in both the mouse (E) and human (F) gut indicates an example of the typical close juxtaposition of NC-derived enteric neurons and vasculature seen with T-cad expression interposed between the two lineages. Scale bar represents 25  $\mu$ m. See [Figure S5](#) to observe the loss of neurovascular co-patterning in the gut of the *T-cad* KO mouse with consequent reduction of NC-derived neurons leading to a condition known clinically as a Hirschsprung's (reduced ganglionic) phenotype. In (C)–(F), the large panel is a merged image of the three markers shown individually as insets at the right of each figure.

## DISCUSSION

By examining neural and vascular co-development in a model of the human epiblast, we offer a mechanism by which such co-patterning emerges and in which primitive BVs then play an active role in early specification and differentiation of neuroectodermal derivatives. Evidence is provided that, of neuroectoderm derivatives, it is the NC, not the NT, that participates in the earliest establishment of this patterning. Also, co-patterning of the migratory NC with the vasculature begins when these cells respond to distinct cues from both the vascular endothelium and smooth muscle to commit to an AN fate. Specifically,

we demonstrate that, for autonomic differentiation, NCs depend on EC-secreted NO and a T-cadherin-mediated homotypic cell-cell interaction with VSMCs. That the vasculature should propel differentiation of the neural cell type most critical for regulating vascular function makes teleological sense. Our finding that the PNS appears to initiate the neurovascular patterning upon which NT-derived CNS neurites come to comport only secondarily adds a new mechanistic perspective to the otherwise old observation of neuronal-vascular co-alignment, which typically has been studied at later stages of development ([Honma et al., 2002](#); [Makita et al., 2008](#); [Mukouyama et al., 2002](#); [Takahashi et al., 2013](#); [Young et al., 2004](#)).

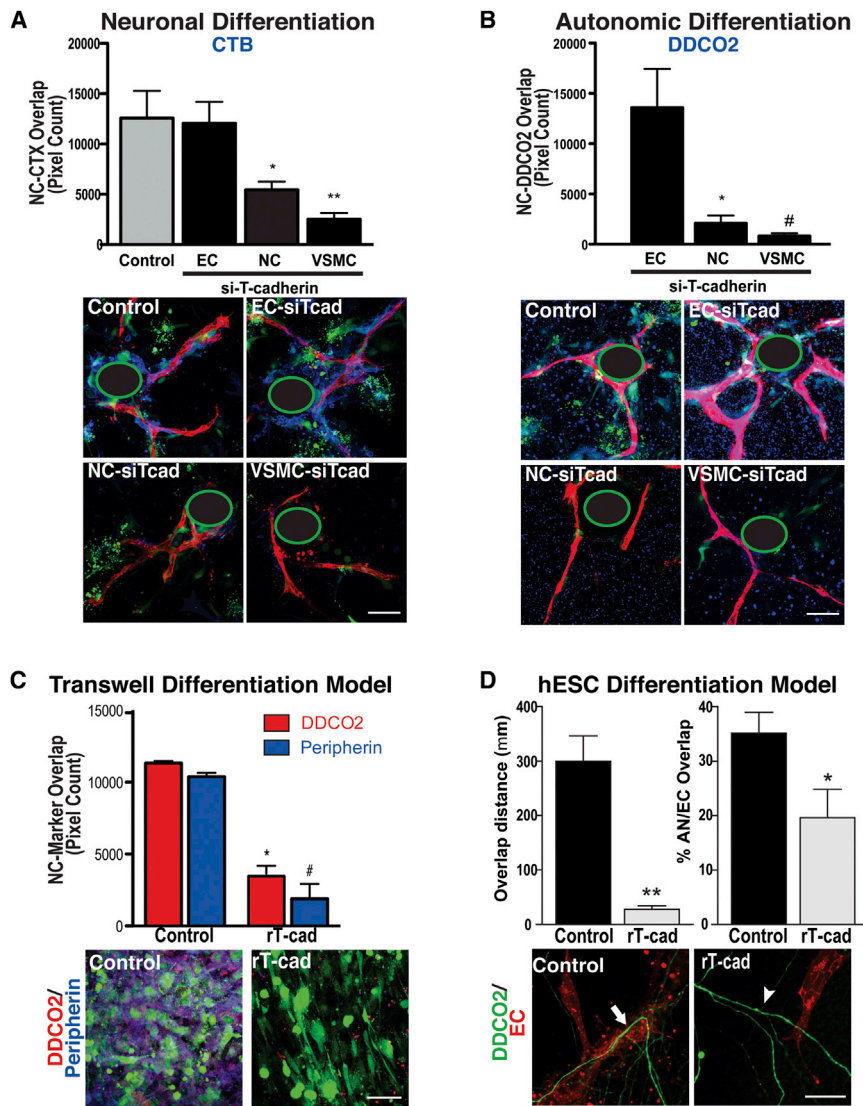


**Figure 6. T-cadherin, Expressed by NCs and VSMCs, Mediates NC Co-alignment and Direct Contact with VSMCs, a Requirement for AN Differentiation**

(A and B) *T-CAD* knockdown in NCs and VSMCs (with siRNA against T-cad [siTcad]) decreased NC (DiI, green) differentiation toward a (A) neuronal fate (CTB, blue) and (B) an AN fate (DDC, blue), as measured by co-localization (overlap of pixels) of NC and marker immunostaining. Knockdown in ECs had no effect. Data are presented as mean  $\pm$  SEM (A, top). For CTB, a one-way ANOVA with Dunnett's post-test was used to determine statistical significance from the control "NC only" group ( $n = 8$  images) ( $n = 11$  images for each siTcad-treated group,  $*p = 0.0164$ ,  $**p = 0.0006$ ). (B, top) For DDC, a one-way ANOVA with Tukey's post-test was used to determine statistical significance from the "NC only" group ( $n = 8$  wells) ( $n = 11$  with three replicates for each siTcad treated group,  $*p = 0.0337$ ,  $\#p = 0.0262$ ). Data are pooled from three independent experiments done in triplicate. (A and B, bottom) Representative images of staining for CTB or DDC. Scale bar represents 100  $\mu$ m. Note that, with the loss of T-cad in NCs and VSMCs, though not in ECs, as a result of siTcad, expression of CTB (blue in A) and DDC (blue in B) is significantly reduced. (The green-encircled black regions represent the location of the Cytodex beads upon which ECs were coated in the 3D fibrin gel system; see Methods). For all experiments, siTcad efficiency was established through real-time PCR by isolating RNA from non-embedded excess cells 48-hr post transfection (Figure S6A).

(C) In the transwell differentiation culture system schematized in Figure 4, addition of recombinant *T-cad* (rT-cad, 1  $\mu$ g/ml), which binds and inhibits T-cad homotypic interaction, to NCs and VSMCs (top chamber), with ECs in the bottom chamber, inhibited NC differentiation toward an AN fate. (Top) Quantitation of DDC (red) and peripherin (blue) staining in NCs (DiI, green) (judged by degree of pixel overlap), treated with control ( $n = 6$  transwells) or rT-cad ( $n = 5$  transwells). Data are presented as mean  $\pm$  SEM and are pooled from three separate experiments. A two-tailed Student's *t* test was used to determine statistical significance.  $*p < 0.0001$ ,  $\#p < 0.0001$ . (Bottom) Representative images of transwells. Scale bar represents 100  $\mu$ m.

(D, top) Percentage of DDC (green) and *U.E.* lectin (red) overlap (right histograms) and length of contact/overlap between ECs and ANs (left histograms) in each image from our hESC differentiation model. A two-tailed Student's *t* test was used to determine statistical significance.  $*p = 0.038$ ,  $**p = 7.5e-6$ , error bars are  $\pm$  SEM;  $n = 9$  images per group from three independent experiments. (Bottom) Representative high magnification images of degree of DDC (green) alignment with ECs (*U.E.* lectin, red) in hESC cultures treated with control versus rT-cad. Scale bar represents 100  $\mu$ m. Note that, in contrast to control conditions (white arrow), with the loss of T-cad action following the addition of rT-cad, NC-derivatives and vasculature no longer co-align (white arrowhead).

NC can differentiate toward a wide range of neural and non-neural cell types. Interaction with other lineages can promote specification (Takahashi et al., 2013); however, the molecular mechanisms that regulate this still remain unclear. Unlike previous studies that focused on the role

of BVs in peripheral and central axon pathfinding (Glebova and Ginty, 2005) and molecular guidance cues (e.g., netrins, artemin, and endothelin) in facilitating co-alignment (Eichmann and Thomas, 2012; Honma et al., 2002), our studies sought to examine human embryogenesis at its



earliest stages, starting with homogeneous pluripotent cells and extending to emergence of the three primitive germ layers as occurs in the epiblast. We were able to discern the role that developing BVs play in NC differentiation. We show that EC-derived NO provides a molecular cue facilitating NC differentiation, consistent with its recognized role in differentiation (Cheng et al., 2003; Reif et al., 2004; Chen et al., 2005; Luo et al., 2010; Oh et al., 2010; Carreira et al., 2012). Specification of NC is then further refined by direct contact with VSMCs via a homotypic T-cad interaction that drives differentiation toward an autonomic neuronal fate. This process is consistent with previous observations that sensory neurons align with immature vessels, whereas sympathetic neurons associate with VSMC-coated vessels (James and Mukoyama, 2011).

T-cad has a previously defined role in regulating the migration and patterning of neuronal and ECs individually (Philippova et al., 2009); our results now reveal a critical role in neurovascular co-patterning and neuronal differentiation. T-cad is an atypical adhesion molecule in that it is a glycosylphosphatidylinositol (GPI)-anchored protein, allowing it to interact with other signaling receptors to promote differentiation. One potential candidate is the receptor tyrosine kinase Ret that is expressed on NCs and promotes autonomic differentiation (Honma et al., 2002). It is therefore not surprising that a Hirschsprung's phenotype (i.e., areas of diminished or absent enteric neurons), which has been tied to Ret deletions in mice and humans, was also observed in the T-cad KO mouse. Interestingly, T-cad has been shown to interact with integrin  $\beta 3$ , which is also expressed by VSMCs during vessel maturation (Scheppke et al., 2012), further suggesting that adhesion to the extracellular matrix plays a role in autonomic differentiation. Therefore, T-cad appears to serve as a molecular bridge facilitating the NC and VSMC contact required for autonomic neuronal differentiation.

Generally, stem cell research focuses on the derivation and differentiation of single lineages in isolation from other cell types. However, the true vertebrate body plan is not constructed in that way. Indeed, most biological processes—starting with the earliest stages of organogenesis in the embryo and extending to organ repair in the adult—demand exquisitely coordinated co-patterning of multiple lineages (often derived from different germ layers) for function to be normal. Neurovascular co-patterning is a prototype for such a developmental program, the cellular and molecular basis for which, at its earliest and most primitive stages in the human epiblast, is actually unknown. By beginning at the earliest stages of human embryogenesis and exploiting hESCs for their value as a model for that primitive developmental period, we identified a fundamental developmental program that drives neuronal fate

determination, ultimately leading to neurovascular formation, and laying a mechanistic basis for the co-patterning observed in more developed or adult organisms. We showed that vascular-mediated neuronal differentiation depends on the maturation state of BVs, defined by the presence of VSMCs. Indeed, the dynamic manner in which the derivatives of these germ layers come to interact and co-pattern may serve as a prototype for how the components of many seemingly unrelated organ systems come to be associated to form the normal human body plan.

## EXPERIMENTAL PROCEDURES

### Cell Culture

Undifferentiated WA09 hESCs were allowed to form EBs and then were seeded onto collagen-coated dishes in order to differentiate, as described previously (Lindquist et al., 2010). Cultures were grown in differentiation media (see Supplemental Experimental Procedures) for up to 28 days. NCs were isolated from hESCs as previously described (Curchoe et al., 2010). Human umbilical vein endothelial cells (HUVECs) and human aortic vascular smooth muscle cells (VSMCs) were cultured as previously described (Scheppke et al., 2012). For live cell imaging, fluorescently labeled *U.E.* lectin and CTB were added to the differentiation media to label vasculature and neurons, respectively.

### 3D Angiogenesis Model

NCs and/or VSMCs were embedded into fibrin gels with or without HUVEC-coated Cytodex beads as previously described (Scheppke et al., 2012). For labeling, NCs were pre-incubated with CellTracker Green or DiIc prior to embedding.

### 2D Co-Culture Assay

NCs ( $1 \times 10^5$  per ml) were seeded onto growth factor-reduced matrigel-coated wells with or without pre-plated HUVECs ( $1 \times 10^6$  per ml) and/or VSMCs ( $1 \times 10^5$  per ml).

### Transwell Assay

NCs labeled as above were plated onto 0.4- $\mu$ m pore transwells coated with growth factor-reduced matrigel. HUVECs and/or VSMCs were plated onto the transwell or bottom chamber. For NO experiments, L-NMMA was added to ECs in the bottom chamber 1 hr after plating. NOC-18 was added to VSMCs and NCs in the upper chamber 1 hr after plating.

### siRNA Studies

For knockdown of *ENOS*, a pool of 4 siRNAs was transfected into ECs 12 hr prior to plating NCs  $\pm$  VSMCs into the top chamber of a transwell. For knockdown of T-cadherin, a pool of 4 siRNAs was similarly transfected into cells 12 hr prior to being embedded in fibrin gels or added to hESC differentiation cultures.

### Analysis of Gut Tissue

Frozen human gastrointestinal (GI) samples were generously provided by Dr. Miguel Reyes-Múgica at the Department of Pathology,



Children's Hospital of Pittsburgh; 5  $\mu$ m cryostat sections were post-fixed in acetone and stained as described in [Supplemental Experimental Procedures](#).

### Pharmacological and Peptide Treatments

Cultures were treated with LM609 ([Scheppke et al., 2012](#)) or control IgG antibody (10  $\mu$ g/ml) from days 16–21. rT-cad ([Fredette et al., 1996](#)) was added to 5  $\mu$ g/ml final concentration as described in the text.

### Immunocytochemistry

Cultures were immunostained as detailed in [Supplemental Experimental Procedures](#). Imaging was performed on a Nikon Spectral C1 confocal microscope. For further details, see [Supplemental Experimental Procedures](#).

### SUPPLEMENTAL INFORMATION

Supplemental Information includes Supplemental Experimental Procedures, six figures, and one movie and can be found with this article online at <http://dx.doi.org/10.1016/j.stemcr.2015.04.013>.

### AUTHOR CONTRIBUTIONS

L.M.A. and J.N.L. designed and performed the experiments, interpreted the data, and wrote the manuscript. C.C., F.C., and A.T. assisted with derivation of NC cells. B.M.W., C.D.P., and P.S. assisted with hESC experiments. B.R. and M.D. assisted with T-cadherin KO experiments. D.A.C. and E.Y.S. supervised the project and assisted with experimental design, data interpretation, and writing the paper.

### ACKNOWLEDGMENTS

We thank Miguel Reyes-Múgica for providing human gut samples. J.N.L. was supported by a training fellowship from the California Institute of Regenerative Medicine (CIRM), and grant support included CIRM-CL1-00511-1 (E.Y.S.), CIRM-RB3-02098 (D.A.C.), NIH-K01CA148897 (L.M.A.), and NIH-P20GM075059 (E.Y.S.).

Received: August 25, 2014

Revised: April 22, 2015

Accepted: April 25, 2015

Published: May 21, 2015

### REFERENCES

Autiero, M., De Smet, F., Claes, F., and Carmeliet, P. (2005). Role of neural guidance signals in blood vessel navigation. *Cardiovasc. Res.* *65*, 629–638.

Carreira, B.P., Carvalho, C.M., and Araújo, I.M. (2012). Regulation of injury-induced neurogenesis by nitric oxide. *Stem Cells Int.* *2012*, 895659.

Chen, J., Zacharek, A., Zhang, C., Jiang, H., Li, Y., Roberts, C., Lu, M., Kapke, A., and Chopp, M. (2005). Endothelial nitric oxide synthase regulates brain-derived neurotrophic factor expression and neurogenesis after stroke in mice. *J. Neurosci.* *25*, 2366–2375.

Cheng, A., Wang, S., Cai, J., Rao, M.S., and Mattson, M.P. (2003). Nitric oxide acts in a positive feedback loop with BDNF to regulate neural progenitor cell proliferation and differentiation in the mammalian brain. *Dev. Biol.* *258*, 319–333.

Cheresh, D.A. (1987). Human endothelial cells synthesize and express an Arg-Gly-Asp-directed adhesion receptor involved in attachment to fibrinogen and von Willebrand factor. *Proc. Natl. Acad. Sci. USA* *84*, 6471–6475.

Curchoe, C.L., Maurer, J., McKeown, S.J., Cattarossi, G., Cimadamore, F., Nilbratt, M., Snyder, E.Y., Bronner-Fraser, M., and Terskikh, A.V. (2010). Early acquisition of neural crest competence during hESCs neuralization. *PLoS ONE* *5*, e13890.

D'Amour, K.A., Agulnick, A.D., Eliazer, S., Kelly, O.G., Kroon, E., and Baetge, E.E. (2005). Efficient differentiation of human embryonic stem cells to definitive endoderm. *Nat. Biotechnol.* *23*, 1534–1541.

Eichmann, A., and Thomas, J.-L. (2012). Molecular Parallels between Neural and Vascular Development (Cold Spring Harbor Perspectives in Medicine).

Fredette, B.J., Miller, J., and Ranscht, B. (1996). Inhibition of motor axon growth by T-cadherin substrata. *Development* *122*, 3163–3171.

Glebova, N.O., and Ginty, D.D. (2005). Growth and survival signals controlling sympathetic nervous system development. *Annu. Rev. Neurosci.* *28*, 191–222.

Halbleib, J.M., and Nelson, W.J. (2006). Cadherins in development: cell adhesion, sorting, and tissue morphogenesis. *Genes Dev.* *20*, 3199–3214.

Hebbard, L.W., Garlatti, M., Young, L.J., Cardiff, R.D., Oshima, R.G., and Ranscht, B. (2008). T-cadherin supports angiogenesis and adiponectin association with the vasculature in a mouse mammary tumor model. *Cancer Res.* *68*, 1407–1416.

Honma, Y., Araki, T., Gianino, S., Bruce, A., Heuckeroth, R., Johnson, E., and Milbrandt, J. (2002). Artemin is a vascular-derived neurotrophic factor for developing sympathetic neurons. *Neuron* *35*, 267–282.

Itskovitz-Eldor, J., Schuldiner, M., Karsenti, D., Eden, A., Yanuka, O., Amit, M., Soreq, H., and Benvenisty, N. (2000). Differentiation of human embryonic stem cells into embryoid bodies compromising the three embryonic germ layers. *Mol. Med.* *6*, 88–95.

Jakobsson, L., Kreuger, J., and Claesson-Welsh, L. (2007). Building blood vessels—stem cell models in vascular biology. *J. Cell Biol.* *177*, 751–755.

James, J.M., and Mukoyama, Y.-S. (2011). Neuronal action on the developing blood vessel pattern. *Semin. Cell Dev. Biol.* *22*, 1019–1027.

Kearney, J.B., and Bautch, V.L. (2003). In vitro differentiation of mouse ES cells: hematopoietic and vascular development. *Methods Enzymol.* *365*, 83–98.

Lindquist, J.N., Cheresh, D.A., and Snyder, E.Y. (2010). Derivation of vasculature from embryonic stem cells. *Curr. Protoc. Stem Cell Biol.* *12*, 1.1F.9.1–1.1F.9.6.

Luo, C.-X., Jin, X., Cao, C.-C., Zhu, M.-M., Wang, B., Chang, L., Zhou, Q.-G., Wu, H.-Y., and Zhu, D.-Y. (2010). Bidirectional



- regulation of neurogenesis by neuronal nitric oxide synthase derived from neurons and neural stem cells. *Stem Cells* 28, 2041–2052.
- Makita, T., Sucov, H.M., Garipey, C.E., Yanagisawa, M., and Ginty, D.D. (2008). Endothelins are vascular-derived axonal guidance cues for developing sympathetic neurons. *Nature* 452, 759–763.
- Mukouyama, Y.S., Shin, D., Britsch, S., Taniguchi, M., and Anderson, D.J. (2002). Sensory nerves determine the pattern of arterial differentiation and blood vessel branching in the skin. *Cell* 109, 693–705.
- Nakatsu, M.N., Davis, J., and Hughes, C.C. (2007). Optimized fibrin gel bead assay for the study of angiogenesis. *J. Vis. Exp.* 3, 186.
- Oh, S.J., Heo, J.I., Kho, Y.J., Kim, J.H., Kang, H.J., Park, S.H., Kim, H.S., Shin, J.Y., Kim, M.J., Kim, S.C., et al. (2010). Nitric oxide is an essential mediator for neuronal differentiation of rat primary cortical neuron cells. *Exp. Neurobiol.* 19, 83–89.
- Philippova, M., Joshi, M.B., Kyriakakis, E., Pfaff, D., Erne, P., and Resink, T.J. (2009). A guide and guard: the many faces of T-cadherin. *Cell. Signal.* 21, 1035–1044.
- Quaeghebeur, A., Lange, C., and Carmeliet, P. (2011). The neurovascular link in health and disease: molecular mechanisms and therapeutic implications. *Neuron* 71, 406–424.
- Reif, A., Schmitt, A., Fritzen, S., Chourbaji, S., Bartsch, C., Urani, A., Wycislo, M., Mössner, R., Sommer, C., Gass, P., and Lesch, K.P. (2004). Differential effect of endothelial nitric oxide synthase (NOS-III) on the regulation of adult neurogenesis and behaviour. *Eur. J. Neurosci.* 20, 885–895.
- Robertson, D.W. (2004). *Primer on the Autonomic Nervous System* (San Diego: Academic Press).
- Rolle, U., Piotrowska, A.P., and Puri, P. (2003). Abnormal vasculature in intestinal neuronal dysplasia. *Pediatr. Surg. Int.* 19, 345–348.
- Scheppke, L., Murphy, E.A., Zarpellon, A., Hofmann, J.J., Merkulova, A., Shields, D.J., Weis, S.M., Byzova, T.V., Ruggeri, Z.M., Iruela-Arispe, M.L., and Cheresch, D.A. (2012). Notch promotes vascular maturation by inducing integrin-mediated smooth muscle cell adhesion to the endothelial basement membrane. *Blood* 119, 2149–2158.
- Suchting, S., Bicknell, R., and Eichmann, A. (2006). Neuronal clues to vascular guidance. *Exp. Cell Res.* 312, 668–675.
- Taguchi, T., Suita, S., Hirata, Y., Hirose, R., Yamada, T., and Toyohara, T. (1994). Abnormally shaped arteries in the intestine of children with Hirschsprung's disease: etiological considerations relating to ischemic theory. *J. Pediatr. Gastroenterol. Nutr.* 18, 200–204.
- Takahashi, Y., Sipp, D., and Enomoto, H. (2013). Tissue interactions in neural crest cell development and disease. *Science* 341, 860–863.
- Tam, S.J., and Watts, R.J. (2010). Connecting vascular and nervous system development: angiogenesis and the blood-brain barrier. *Annu. Rev. Neurosci.* 33, 379–408.
- Thomson, J.A., Itskovitz-Eldor, J., Shapiro, S.S., Waknitz, M.A., Swiergiel, J.J., Marshall, V.S., and Jones, J.M. (1998). Embryonic stem cell lines derived from human blastocysts. *Science* 282, 1145–1147.
- Wang, R., Clark, R., and Bautch, V.L. (1992). Embryonic stem cell-derived cystic embryoid bodies form vascular channels: an in vitro model of blood vessel development. *Development* 114, 303–316.
- Young, H.M., Anderson, R.B., and Anderson, C.R. (2004). Guidance cues involved in the development of the peripheral autonomic nervous system. *Auton. Neurosci.* 112, 1–14.
- Zacchigna, S., Ruiz de Almodovar, C., and Carmeliet, P. (2008). Similarities between angiogenesis and neural development: what small animal models can tell us. *Curr. Top. Dev. Biol.* 80, 1–55.